



## A new assay for quantitative detection of hepatitis A virus

Sofia Persson<sup>a,b,\*</sup>, Erik Alm<sup>c</sup>, Måns Karlsson<sup>d</sup>, Theresa Enkirch<sup>e</sup>, Heléne Norder<sup>f,g</sup>,  
Ronnie Eriksson<sup>a</sup>, Magnus Simonsson<sup>a</sup>, Patrik Ellström<sup>b</sup>

<sup>a</sup> European Union Reference Laboratory (EURL) for Foodborne Viruses, Swedish Food Agency, Box 622, SE-751 26, Uppsala, Sweden

<sup>b</sup> Department of Medical Sciences, Zoonosis Science Centre, Uppsala University, Husargatan 3, SE-751 23, Uppsala, Sweden

<sup>c</sup> Unit for Laboratory Development, Department of Microbiology, The Public Health Agency of Sweden, Nobels väg 18, SE-171 65, Solna, Sweden

<sup>d</sup> Department of Mathematics, Stockholm University, SE-106 91, Stockholm, Sweden

<sup>e</sup> Unit for Laboratory Surveillance of Viral Pathogens and Vaccine Preventable Diseases, Department of Microbiology, The Public Health Agency of Sweden, Nobels väg 18, SE-171 65, Solna, Sweden

<sup>f</sup> Department of Infectious Diseases, Institute of Biomedicine at Sahlgrenska Academy, University of Gothenburg, SE-413 46, Gothenburg, Sweden

<sup>g</sup> Region Västra Götaland, Sahlgrenska University Hospital, Department of Clinical Microbiology, SE-413 45 Gothenburg, Sweden

### ARTICLE INFO

#### Keywords:

Hepatitis A virus  
Digital PCR  
Real-time PCR  
Reverse transcription  
Validation  
Food-borne virus

### ABSTRACT

Hepatitis A virus (HAV) is mainly transmitted via contaminated food or water or through person-to-person contact. Here, we describe development and evaluation of a reverse transcription droplet digital PCR (RT-ddPCR) and reverse transcription real-time PCR (RT-qPCR) assay for detection of HAV in food and clinical specimens. The assay was evaluated by assessing limit of detection, precision, matrix effects, sensitivity and quantitative agreement. The 95 % limit of detection (LOD95 %) was 10 % higher for RT-ddPCR than for RT-qPCR. A Bayesian model was used to estimate precision on different target concentrations. From this, we found that RT-ddPCR had somewhat greater precision than RT-qPCR within runs and markedly greater precision between runs. By analysing serum from naturally infected persons and a naturally contaminated food sample, we found that the two methods agreed well in quantification and had comparable sensitivities. Tests with artificially contaminated food samples revealed that neither RT-ddPCR nor RT-qPCR was severely inhibited by presence of oysters, raspberries, blueberries or leafy-green vegetables. For this assay, we conclude that RT-qPCR should be considered if rapid, qualitative detection is the main interest and that RT-ddPCR should be considered if precise quantification is the main interest. The high precision of RT-ddPCR allows for detection of small changes in viral concentration over time, which has direct implications for both food control and clinical studies.

### 1. Introduction

Hepatitis A virus (HAV) is a major cause of acute viral hepatitis (Murray et al., 2015). The virus belongs to the *Hepatitisvirus* genus of the *Picornaviridae* family and the genome consists of a positive-sense, single-stranded RNA molecule of 7.5 kilobases with a single open reading frame (ORF) flanked by 3' and 5' untranslated regions (UTRs). The human HAV strains are classified in three genotypes (I, II and III) and seven subtypes (IA, IB, IC, IIA, IIB, IIIA and IIIB) (Pérez-Sautu et al., 2011; Pintó et al., 2012). Worldwide, subtype IA is the most prevalent, but strains of subtype IIIA, which are dominant in South Asia (D'Andrea et al., 2015), seem to spread rapidly to other parts of the world (Bosch et al., 2016; Miyamura et al., 2012; Mukomolov et al., 2012). Transmission of HAV occurs mainly via the faecal-oral route through ingestion

of contaminated food or water, or directly from person-to-person (Martin and Lemon, 2006; Mast and Alter, 1993; Murray et al., 2015). Foods previously associated with HAV outbreaks include oysters and clams (Costafreda et al., 2006; Sánchez et al., 2002), strawberries (Enkirch et al., 2018; Nordic, 2013; Scavia et al., 2017), raspberries (Hutin et al., 1999; Reid and Robinson, 1987), blueberries (Calder et al., 2003), dates (Rajjuddin et al., 2018), leafy green vegetables (Callejón et al., 2015; Herman et al., 2015; Rosenblum et al., 1990) and semi-dried tomatoes (Carvalho et al., 2012; Petriagnani et al., 2010).

Reverse transcription quantitative real-time PCR (RT-qPCR) is the standard method for quantitative detection of HAV in food, as described in ISO 15216–1 (Microbiology of the food chain - Horizontal method for determination of hepatitis A virus and norovirus using real-time RT-PCR - Part 1: Method for quantification, hereafter referred to as the 'ISO

\* Corresponding author at: Swedish Food Agency, Box 622, SE-751 26 Uppsala, Sweden.

E-mail address: [sofia.persson@slv.se](mailto:sofia.persson@slv.se) (S. Persson).

<https://doi.org/10.1016/j.jviromet.2020.114010>

Received 10 June 2020; Received in revised form 19 October 2020; Accepted 30 October 2020

Available online 2 November 2020

0166-0934/© 2020 The Authors. Published by Elsevier B.V. This is an open access article under the CC BY license (<http://creativecommons.org/licenses/by/4.0/>).

method') (ISO, 2017). Clinical diagnosis of hepatitis A is mainly based on enzyme immunoassays for detection of anti-HAV immunoglobulin M (IgM) in serum, but a quantitative RT-PCR method can be used as a complement to monitor viremia and faecal shedding of the virus (Nainan et al., 2006). Viremia starts up to 30 days before the onset of symptoms and several days before IgM antibodies can be detected in serum (Bower et al., 2000; Nainan et al., 2006). Faecal shedding of HAV reaches its peak just before symptoms appear, and this is the time when the infected individual is most contagious (Pintó et al., 2012).

Broad diagnostic RT-PCR testing for RNA viruses can be challenging due to sequence heterogeneity between strains. Although HAV displays a relatively high degree of nucleotide conservation (Nainan et al., 2006) in comparison with many other RNA viruses, we recently reported that the HAV assay recommended in the ISO method (ISO, 2017) underestimates the target concentration and has an impaired limit of detection of HAV genotype III strains due to primer-template mismatches (Persson et al., 2019). In addition, food and water samples often contain inhibitors of reverse transcription and/or PCR (Schrader et al., 2012), causing underestimation of the target concentration or false negative results. Reverse transcription droplet digital PCR (RT-ddPCR) is increasingly being used as an alternative or complement to RT-qPCR. In comparison with RT-qPCR, RT-ddPCR generally provides greater precision of quantification (Hayden et al., 2013; Hindson et al., 2013; Persson et al., 2018) and under some circumstances is also less affected by inhibitory substances (Coudray-Meunier et al., 2015; Racki et al., 2014) and primer-template mismatches (Persson et al., 2019; Sedlak et al., 2017; Strain et al., 2013).

To overcome the limitation with the assay recommended in the ISO method (ISO, 2017; Persson et al., 2019), we developed a new assay for detection of HAV in food and clinical samples, designed for onestep RT-ddPCR and one-step RT-qPCR. The assay is designed to detect strains of HAV genotypes I, II and III, and is targeted to a conserved region within the 5' untranslated region (UTR). The selectivity of the assay was determined *in silico*, and experimental evaluation was performed to determine 95 % limit of detection (LOD95 %), linearity and precision of quantification. Matrix effects were investigated by analysing food sample extracts spiked with viral RNA from HAV. Sensitivity and quantitative agreement between RT-ddPCR and RT-qPCR were evaluated by analysing food and clinical serum samples known to be positive for HAV. Lastly, the new assay was compared with the assay suggested in the ISO method (ISO, 2017), by measuring RT-qPCR performance and LOD.

## 2. Materials and methods

### 2.1. Ethical considerations

De-identified patient serum and plasma samples previously collected for the purpose of clinical diagnosis of HAV were used for assay development and quality assurance, in accordance with local guidelines. Such activities are not subject to review according to the Swedish Act concerning the Ethical Review of Research Involving Humans (2003:460), and hence no ethical approval was required.

**Table 1**

Primer and probe sequences used in the new assay.

Type	Sequence (5'-3')	Sense	Position (within NC001489)	Length (nt)	% GC	T <sub>m</sub> (°C) <sup>a</sup>	Reference
Forward	CTCTTTGATCTTCCACAAGRGGT	+	373–395	23	45.7	55.3 and 56.8	This study
Reverse	GCCGCTGTATCCCTATCCAA	–	444–463	20	55	58.2	(Jiang et al., 2014; Persson et al., 2019; Win et al., 2019)
Probe	FAM-AGGCTACGGGTGAAAC-MGB-EQ	+	396–411	16	56.3	Not assessed	This study

FAM = 6 carboxyfluorescein, MGB-EQ = minor groove binder-eclipse quencher.

<sup>a</sup> Calculated using OligoAnalyzer Tool 3.1 (Integrated DNA Technologies, Iowa, United States), using an Na<sup>+</sup> concentration of 50 mM and an oligo concentration of 500 nM.

### 2.2. Assay design

The primers and probe (Table 1) were designed using in-house software ('SMI designer') developed at the Public Health Agency, Stockholm, Sweden. The most suitable target region was determined by visually inspecting sequence conservation (see Section 2.4) together with primer and probe melting temperatures, GC-content, amplicon length and primer dimer alignments.

### 2.3. Collection of HAV sequences from GenBank

Hepatitis A virus sequences were collected from GenBank using the query "A"[porgn:\_txid12092] NOT modified[TITLE] NOT patent [TITLE]. The search had 8127 hits (as of November 11, 2018). All sequences were genotyped using Hepatitis A Virus Genotyping Tool version 1.0 (<https://www.rivm.nl/mpf/typingtool/hav/>, accessed November 26, 2018). Sequences belonging to genotypes other than I, II and III and sequences that could not be identified as HAV were removed from the dataset, resulting in 8051 remaining sequences. Among these, there were 67 complete genome sequences (longer than 7450 nucleotides) and 487 sequences that contained the amplicon region of the assay.

### 2.4. Alignment and analysis of complete genomes

All sequences longer than 7450 nucleotides ( $n = 67$ ) were aligned using Muscle (Edgar, 2004) to identify conserved regions of the genome. The alignment was imported to R 4.0.0 (R, 2020) using the *read.alignment* function in the *seqinr* package (Charif and Lobry, 2007). The consensus sequence, guanine-cytosine (GC) content, Shannon entropy [a measurement of sequence variability (Shannon, 1951)] and the nucleotide frequency at each site were retrieved using in-house functions. Sites with at least 50 % gaps were removed. Centered running averages for GC content, Shannon entropy and nucleotide identity (proportion of the most common base at each position) were also calculated using in-house functions.

### 2.5. *In silico* selectivity

#### 2.5.1. Inclusivity

Inclusivity was referred to as the ability of an assay to detect target sequences of interest (Hedman et al., 2018). For our assay, this primarily included strains of HAV genotypes I, II and III. Sequences of interest containing the amplicon region ( $n = 487$ ) were aligned with primer and probe sequences using Muscle (Edgar, 2004). The assay was also matched against simian HAV [genotypes IV, V and VI (Lemon et al., 1992)]. Nine sequences of HAV genotype V that covered the amplicon region were found, but no sequences of genotypes IV and VI, which means that genotype V was the only simian genotype that could be assessed.

### 2.5.2. Exclusivity

Exclusivity was referred to as the ability of an assay to avoid detecting sequences of non-interest (Hedman et al., 2018). To identify sequences of non-interest that could potentially be amplified by the assay, the primer and probe sequences were matched separately towards sequences of non-interest in the NCBI nucleotide collection database. The HAV taxonomy ID (12,092) was excluded and blastn was performed with the following exceptions to the default settings: Expect threshold: 1000, word size: 7, match/mismatch scores: +1/-1. Accession numbers were extracted from each hit table and intersects were calculated using the *intersect* function in R 4.0.0 (R, 2020), to identify accession numbers that occurred in all three hit tables (forward primer, reverse primer and probe). These sequences were downloaded and investigated manually for risk of amplification.

### 2.6. Generation of a DNA quantification standard for RT-qPCR and external control RNA

A sequence corresponding to nucleotide 1–542 of the HAV genome (NC001489) with an upstream T7 promoter and a downstream *Hind*III restriction site was ligated into a pEX-A2 vector (Eurofins Genomics, Ebersberg, Germany). The plasmid was linearised with *Hind*III (New England Biolabs, Ipswich, United States) and separated by 1 % agarose gel (Sigma Aldrich, Saint Louis, United States) electrophoresis at 100 V for 2.5 h. The linear gel band was excised and purified with QIAquick® Gel Extraction Kit (Qiagen, Hilden, Germany). External control (EC) RNA for monitoring the inhibitory effect was generated using Riboprobe® Combination System T7 RNA Polymerase (Promega, Madison, United States) and then DNase-treated according to the manufacturer's protocol. Clean-up of transcripts was carried out with an RNeasy MinElute Cleanup Kit (Qiagen). All transcripts were quality controlled using qPCR with and without reverse transcription, to ensure that the DNA content was below 0.1 %. Quantification of plasmids and transcripts was conducted using a Qubit® 3.0 Fluorometer together with the appropriate kit (Qubit® dsDNA HS kit or Qubit® RNA HS kit) (Thermo Fisher Scientific, Waltham, United States). The material was diluted to appropriate concentrations in 1X TE buffer (Sigma Aldrich, Saint Louis, United States), split into single-use aliquots and stored at -70 °C.

### 2.7. RNA extraction

Viral RNA was extracted with NucliSENS® miniMAG® (bioMérieux, Marcy l'Etoile, France) according to the manufacturer's instructions. The sample volume was between 100 and 500 µL and the elution volume was 100 µL. A negative extraction control with PBS (phosphate buffered saline) was included in each extraction round. Eluates were stored as single-use aliquots at -70 °C.

### 2.8. RT-ddPCR

One-step RT-ddPCR was performed using the One-Step RT-ddPCR Advanced Kit for Probes (Bio-Rad, Hercules, United States). The reaction mix contained 500 nM forward primer, 900 nM reverse primer and 150 nM probe. Each sample (5.5 µL template and 16.5 µL reaction mix) was first applied to a 96-well plate with a final volume of 22 µL (20 µL + 10 %). Then 20 µL of each sample were transferred to DG8™ Cartridges (BioRad), and 70 µL of Droplet Generation Oil for Probes were added (Bio-Rad). Droplets were generated with a QX200™ Droplet Generator (BioRad). Next, 40 µL droplet suspension were transferred to a 96-well plate (Eppendorf, Hamburg, Germany). RT-PCR was performed in a T100™ Thermal Cycler (Bio-Rad) with RT at 50 °C for 1 h, inactivation of the reverse transcriptase and DNA polymerase activation at 95 °C for 10 min, followed by 50 cycles of denaturation at 95 °C for 30 s, and annealing/elongation at 60 °C for 1 min. A final enzyme deactivation step was performed at 98 °C for 10 min. Plates were transferred to the QX200™ Droplet Digital™ PCR system (Bio-Rad) on

the same day or the day after the reaction. Results were visualised in QuantaSoft™ Analysis Pro software version 1.0 (BioRad). A fixed threshold at 4000 relative fluorescence units was used throughout the study. A checklist from digital MIQE guidelines (minimum information for publication of digital PCR experiments) (Huggett et al., 2013) is provided in Table S1 in Supplementary Material.

### 2.9. RT-qPCR

One-step RT-qPCR was performed with the RNA UltraSense™ One-Step Quantitative RT-PCR System (Thermo Fisher Scientific) on a LightCycler® 96 System (Roche, Basel, Switzerland). Each reaction contained 500 nM forward primer, 900 nM reverse primer and 150 nM probe. For each sample, a total of 25 µL reaction mix was prepared with 20 µL of reagents and 5.0 µL of sample. RT-qPCR was performed with RT at 55 °C for 1 h, inactivation of the reverse transcriptase and activation of the DNA polymerase at 95 °C for 5 min, followed by 45 cycles of denaturation at 95 °C for 15 s, annealing at 60 °C for 1 min, and elongation at 65 °C for 1 min. Results were analysed with the LightCycler® 96 software, version 1.1 (Roche). Quantification was performed using a 10-fold dilution series of linearised plasmid DNA. The calibration curve ranged from 10<sup>4</sup> to 10 plasmid equivalents per reaction in the evaluation study (for reasons of space on the PCR plate) and from 10<sup>5</sup> to 10 plasmid equivalents per reaction in all other experiments. A checklist from MIQE guidelines (minimum information for publication of quantitative real-time PCR experiments) (Bustin et al., 2009) is provided in Table S2 in Supplementary Material.

### 2.10. Assessment of LOD95 %, linearity and precision

#### 2.10.1. Study design

A two-fold dilution series, ranging from neat to 1/512 dilution, was prepared with viral RNA from HAV HMI175/18f (ATCC® VR-1402™, Manassas, United States, accession number M59808). The RNA was diluted in 1X TE buffer (Sigma Aldrich, Saint Louis, United States), split into single-use aliquots and stored at -70 °C until use. For each of the two methods (RT-ddPCR and RT-qPCR), the 10 different dilution levels were tested in four different runs, with eight replicate sample wells per dilution level and run, resulting in 320 RT-PCR wells per method. Eight no-template controls (NTCs) were also included in each run. The experiments were performed under repeatability conditions (ISO, 1994), i. e. during a short period of time, within the same laboratory, by the same analyst and using the same equipment, conditions and material. Anticipated concentration was calculated by taking the mean of the measurements (log<sub>2</sub> concentration) at the undiluted level of each method, followed by subtraction of one for each dilution level.

#### 2.10.2. Probability of detection and LOD95 %

The 95 % limit of detection (LOD95 %) was determined for RT-ddPCR and RT-qPCR. For this purpose, a logistic regression model (Model 1) was fitted with probability of detection as a function of anticipated concentration (log<sub>2</sub> scale). One model was fitted for RT-ddPCR and one for RT-qPCR. The LOD95 % is the lowest anticipated target concentration that can be detected with 95 % probability (Forootan et al., 2017).

To compare the performance of RT-ddPCR and RT-qPCR in terms of qualitative detection, a multiple logistic regression model (Model 2) was fitted with probability of detection as a function of dilution level (log<sub>2</sub> scale) and method. An interaction term between dilution level and method was included to allow for direct comparison with Model 1. The unknown model parameters were estimated using the *glm* function in R 4.0.0 (R, 2020). An effect was considered significant at  $p \leq 0.05$ .

#### 2.10.3. Linearity and precision

All dilutions with an anticipated concentration higher than LOD95 % were assessed for linearity and precision (variability in measurements,

expressed as a SD). Linearity was assessed visually by plotting  $\log_2$  measured concentration against  $\log_2$  anticipated concentration. Precision was then assessed for each method across all anticipated concentrations higher than LOD95 %, for which linearity could safely be assumed. Statistically, this would have been a rather standard task if homogeneity of the error terms could be assumed. However, due to Poisson sampling error (Matz et al., 2013), the variance in PCR data (on log scale) is expected to increase as the template concentration decreases. Hence, instead of using a classical linear mixed model with a homogeneity assumption on the residual variance, we chose a Bayesian model (Model 3) and created a predictor not only for the expected value of the response (measured concentration), but also for the SD of the error terms, to better take the nature of PCR data into account.

The aim was to assess precision of quantification both within and between runs. For this reason, run was included as a grouping factor in the model, and both the intercept and the slope of anticipated concentration were allowed to vary between runs. In this regard, the model was essentially a linear mixed effects model, with a random intercept and slope for each run. However, as mentioned, we also created a predictor for the residual term SD (which amounts to the within-run SD), to encompass the heterogeneity. Thus, the between-run variation was assessed in terms of two aspects (how much the intercept varied and how much the slope varied), while accounting for heterogeneity. The model is summarised below.

For all observations  $i = 1, \dots, N$  we introduce the following notation

$y_i$  - the *measured concentration* ( $\log_2$  scale, continuous number) of observation  $i$

$x_i$  - the *anticipated concentration* ( $\log_2$  scale, continuous number) of observation  $i$

$run_i$  - to which *run* observation  $i$  belongs, i.e. this is a grouping factor that ranges from 1 to 4

and present the following general model:

$$y_i \sim N(\mu_i, \sigma_i)$$

$$\mu_i = \alpha + \delta_{1run_i} + (\beta + \delta_{2run_i}) \cdot x_i,$$

$$\sigma_i = \eta / x_i$$

$$\delta_{1run_i} \sim N(0, \sigma_{\delta_1}) \quad \delta_{2run_i} \sim N(0, \sigma_{\delta_2})$$

$$\sum_{j=1}^4 \delta_{1j} \sim N(0, 0.04) \quad \sum_{j=1}^4 \delta_{2j} \sim N(0, 0.04)$$

The last row is a soft constraint on the intercept and slope shifts to sum to zero. The parameters, what we know about them a priori and the prior distributions we impose, are:

$\alpha$  - the overall intercept, should be close to zero,  $N(0, 1)$  -prior

$\delta_{1run_i}$  - the intercept shift for  $run_i$ , should be quite close to zero.  $N(0, \sigma_{\delta_1})$  -prior, as specified above.

$\beta$  - the overall slope parameter of *anticipated concentration*, should be close to one.  $N(1, 1)$  -prior.

$\delta_{2run_i}$  - the slope shift for  $run_i$ , should be quite close to zero.  $N(0, \sigma_{\delta_2})$  -prior, as specified above.

$\sigma_{\delta_1}$  - the SD of the intercept shifts; positive,  $C(0, 2)$  prior

$\sigma_{\delta_2}$  - the SD of the slope shifts; positive,  $C(0, 2)$  -prior.

$\eta$  - the expected within-run SD when *anticipated concentration* is 1. We know from past experience that the variance increases as *anticipated concentration* decreases. Since  $\sigma_i$  is a variance parameter for  $i = 1, \dots, N$  it must be larger than zero, and as there are only positive values of  $x_i$  in the model,  $\eta$  must be positive. It is important to note that a restriction of our model is that it only holds for positive  $x_i$  -values.  $U(0, \infty)$  -prior, i.e. a flat prior.

$\mu_i$  - the expected value of *measured concentration* for observation  $i$

$\sigma_i$  - the expected SD of *measured concentration* for observation  $i$

One model was fitted for RT-ddPCR and one for RT-qPCR. The

performance characteristics of the two methods were then compared through approximations of the posterior distributions of the model parameters. Samples from the posterior distributions were generated using Markov Chain Monte Carlo (MCMC), by implementing the model in Stan (Carpenter et al., 2017) and accessing it via the R 4.0.0 (R, 2020) interface rstan (Stan, 2020). Diagnostics of the MCMC of Stan for Model 3 are shown in Fig. S1 in Supplementary Material.

### 2.11. Matrix effects

Nucleic acid extracts of oysters, raspberries, blueberries and leafy green vegetables were prepared according to the instructions in ISO 15216-1 (ISO, 2017). For each food type, one 25 g sample was prepared, and four replicate wells containing 5.0  $\mu$ L of food sample nucleic extract were spiked with 2.0  $\mu$ L of viral RNA from HAV HM175/18f (ATCC® VR-1402™, accession number M59808) at a concentration of 1000 copies per reaction. Two replicate wells of unspiked food sample were included to confirm that the food sample was negative for HAV. The wells containing food sample and viral RNA ('sample wells') were compared with four wells containing 5.0  $\mu$ L molecular-grade water (Qiagen) spiked with an equal amount of viral RNA ('control wells'). The matrix effect was considered acceptable if it was less than 75 % (ISO, 2017) (i.e. the amount of EC RNA detected in the sample well was at least 25 % of that detected in the control well). It was also of interest in this study to examine whether the matrix effect differed if an end-point or a real-time detection technique was used. As RT-ddPCR and RT-qPCR had different kits and reaction conditions, the conditions described for RT-ddPCR (enzyme kit, volume and thermal profile) were evaluated on the qPCR platform as a control, to allow for more direct comparison of the detection techniques.

### 2.12. Sensitivity and quantitative agreement

#### 2.12.1. Sample collection and preparation

A set of 37 human serum specimens from patients diagnosed with hepatitis A by the presence of anti-HAV IgM and viral RNA was obtained from the Public Health Agency, Stockholm, Sweden, and Sahlgrenska University Hospital, Gothenburg, Sweden. These samples were collected in hospital and primary care settings between 2013 and 2018. In addition, 14 plasma samples with varying concentrations of HAV obtained from the Quality Control for Molecular Diagnostics (QCMD) HAV panel 2017 and 2018 for External Quality Assessment (EQA) were used for verification (<https://www.qcmd.org/>, accessed August 16, 2019). A 100  $\mu$ L volume of each sample was extracted as described in the section 'RNA Extraction'. A naturally contaminated strawberry sample containing HAV genotype IB (Enkirch et al., 2018) was also included. The strawberry sample was extracted as described in ISO 15216-1 (ISO, 2017). All samples were analysed in duplicate as described in the sections 'RT-ddPCR' and 'RT-qPCR', and the concentrations were  $\log_{10}$ -transformed before further analysis. To monitor the inhibitory effect, a sample spiked with 2.0  $\mu$ L of EC RNA (corresponding to  $10^4$  copies) was analysed and compared with a control well containing 2.0  $\mu$ L of EC RNA and nuclease-free water. The 95 % confidence intervals (CI) for the mean inhibitory effect were obtained from the  $t$ -distribution, using the  $t.test$  function in R 4.0.0 (R, 2020).

#### 2.12.2. Sensitivity

Sensitivity was determined as the probability of a positive result, given that the sample contained HAV RNA. The presence of HAV RNA in the samples was previously determined by qualitative RT-PCR analysis using a protocol derived from (HAVNet, 2018) followed by gel electrophoresis, sequencing and genotyping (genotype IA  $n = 9$ , IB  $n = 26$ , IIA  $n = 4$  and IIIA  $n = 13$ ). The sensitivity was estimated by dividing the number of positive samples by the total number of samples ( $n = 52$ ), and multiplying by 100. The 95 % CI for the percentage of positive samples were obtained using the  $prop.test$  function in R 4.0.0 (R, 2020).

### 2.12.3. Quantitative agreement

Quantitative agreement between RT-ddPCR and RT-qPCR was determined using the Bland and Altman method (Bland and Altman, 1986). Systematic bias was estimated by taking the mean of the difference in  $\log_{10}$  concentration between RT-ddPCR and RT-qPCR of each sample that provided a positive test result with both methods.

### 2.13. Comparison with a standard method

The assay developed in this study was compared with the assay described in ISO 15216–1 (ISO, 2017), also with a FAM-fluorophore, by analysing *in vitro*-transcribed RNA template (see section ‘Generation of a DNA quantification standard for RT-qPCR and external control RNA’) in RT-qPCR (see section ‘RT-qPCR’). The assay performance was evaluated by examining the amplification curves with and without the presence of RNA extract from a raspberry sample (a representative food matrix, as described in the section ‘Matrix effects’). A rough estimate of LOD was obtained by analysing a 10-fold serial dilution of *in vitro*-transcribed RNA template, with four wells per dilution level.

## 3. Results

### 3.1. Analysis of complete genomes and assay position

Analysis of 67 complete HAV genomes verified that 5' UTR was the most conserved region of the genome (Fig. 1). The combined analysis of sequence conservation and optimal oligo properties (GC-content, amplicon length, melting temperatures and primer-dimer alignments) identified an assay targeted to nucleotide 373–463 within the 5' UTR (as determined from the HAV reference genome, NC001489) as the most suitable candidate (Table 1). The reverse primer has been published previously (Jiang et al., 2014; Win et al., 2019). This region represents one of the most conserved regions of the entire genome; all 20 nucleotides had at least 97 % similarity (Fig. 1),

### 3.2. *In silico* inclusivity

Of all sequences containing the entire amplicon region ( $n = 487$ ), which was 91 nucleotides long in all cases, the assay matched perfectly with 370 (76 %) (Table 2). A particularly common mismatch among genotype III sequences was a single C (primer) to A (template) mismatch located at the third nucleotide from the 5' end of the forward primer. One sequence with potentially severe mismatches was identified (AB045668.1), with two mismatches at the probe region (positions 2

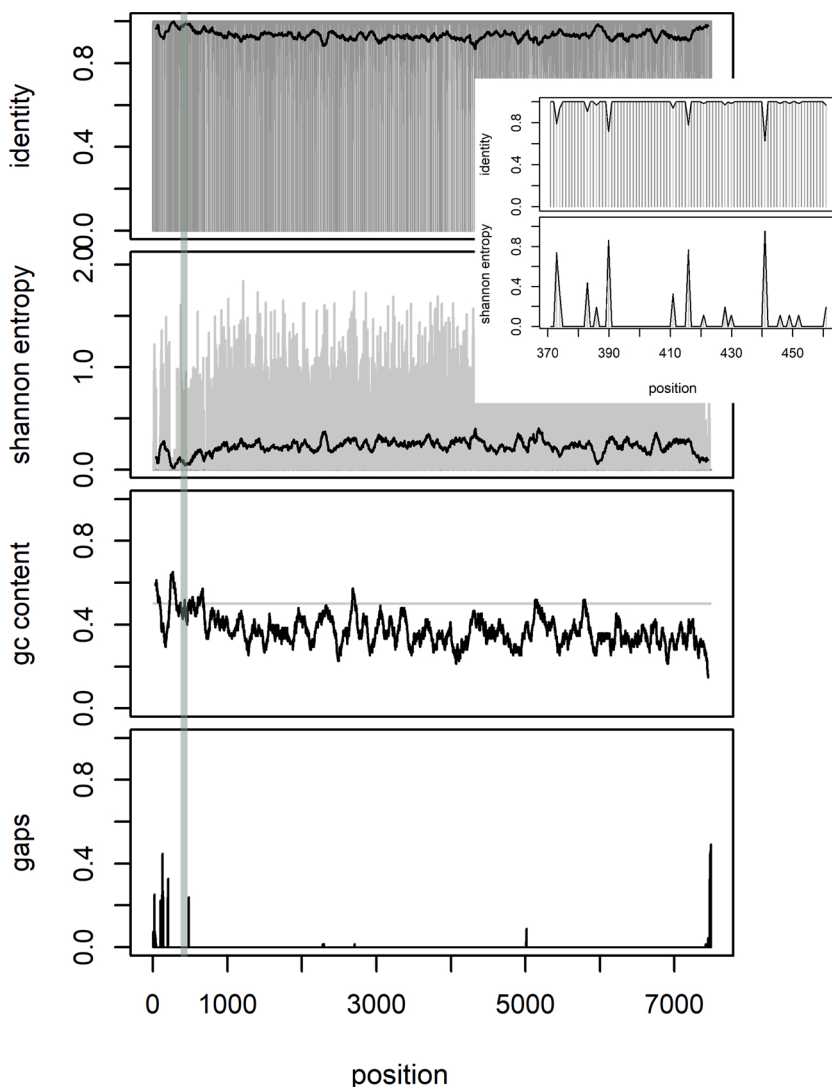


**Fig. 1.** Nucleotide identity, Shannon entropy (a measurement of variability; a value of zero indicates no variability and a high value indicates high variability), GC content and gap frequency based on alignment of 67 complete hepatitis A virus (HAV) genome sequences. Horizontal lines represent centred running averages and the vertical bars represent the value at each position. Black bars in the two uppermost figures represent values of 1 and 0, respectively (i.e. positions with complete conservation). The shaded area indicates the amplicon region. The small figure illustrates nucleotide identity and Shannon entropy within the amplicon region.

**Table 2**

Summary of results of *in silico* inclusivity analysis. Number of perfectly matching sequences/total number of sequences.

Genotype	Forward primer	Probe	Reverse primer	Complete assay
I	160/181	180/181	174/181	155/181
II	4/4	4/4	4/4	4/4
III	1/52	52/52	50/52	1/52
Unassigned	222/250	246/250	229/250	210/250
Total	387/487	481/487	457/487	370/487

and 14 from the 5' end) and two at the 3' end of the reverse primer region (positions 13 and 14). The genotype of that sequence could not be determined. The primer and probe sequences matched moderately well with HAV genotype V (a simian genotype), suggesting that amplification may occur if the genotype is present in the sample.

### 3.3. *In silico* exclusivity

No sequence that could produce an amplicon was found when blasting primer and probe sequences to non-HAV sequences with loose match criteria, suggesting that cross reactivity is unlikely.

### 3.4. No template controls

In RT-ddPCR, one of the 32 NTCs contained one positive droplet. In RT-qPCR, none of the 32 NTCs had a Cq value. Based on these results, a sample was defined as positive when it had at least one positive droplet in RT-ddPCR and a Cq value in RT-qPCR.

### 3.5. Probability of detection and LOD95 %

A dilution series of viral RNA from HAV was analysed using RT-ddPCR and RT-qPCR and evaluated for qualitative detection. From Model 1, it was found that LOD95 % was 6.1 copies per reaction for RT-ddPCR and 3.0 copies per reaction for RT-qPCR (Fig. 2). These numbers are not directly comparable, as the two methods differed in quantification. The neat samples provided a geometric mean of 293 copies/reaction with RT-ddPCR and 166 copies/reaction with RT-qPCR, which means that the anticipated concentration was about 1.8-fold higher in RT-ddPCR than in RT-qPCR. Model 2 enabled direct comparison by having dilution level as an explanatory variable, instead of anticipated concentration. It was found that the probability of detection was higher with RT-qPCR than RT-ddPCR ( $p = 0.05$ ). The difference in LOD95 % was 0.19 dilution levels, meaning that LOD95 % occurred at  $2^{0.19} = 1.1$ -fold (10 %) higher template concentration for RT-ddPCR than for RT-qPCR (visualised in Fig. S2 in Supplementary Material).

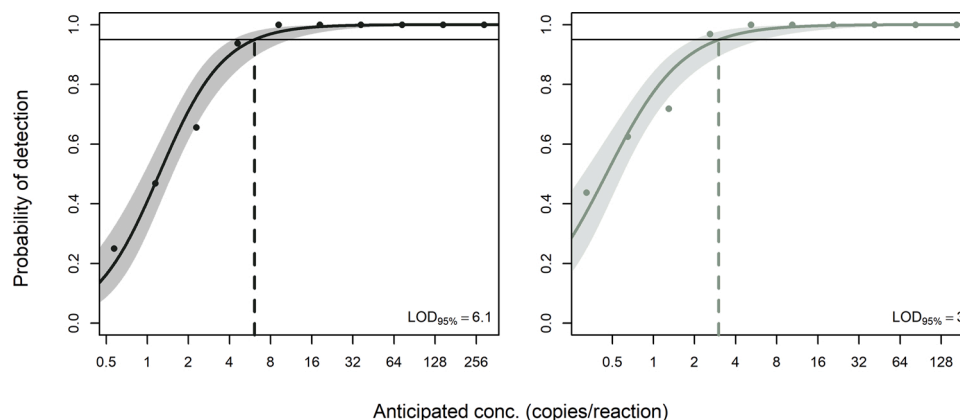


**Fig. 2.** Qualitative detection: Probability of detection versus anticipated concentration. The dots represent observed values, the solid line represents the predicted mean and the coloured area indicates 95 % confidence interval (CI) for the predicted mean. Left: RT-ddPCR, right: RT-qPCR.

### 3.6. Linearity and precision

A dilution series of viral RNA from HAV was analysed using RT-ddPCR and RT-qPCR and evaluated for quantitative detection. A linear response was confirmed across all dilution levels with an anticipated concentration higher than LOD95 %, which were the six most concentrated dilution levels for both methods. These dilution levels were included in Model 3 for analysis of precision. In anticipated concentration, this corresponded to 9.2–293 copies/reaction in RT-ddPCR and 5.2–166 copies/reaction in RT-qPCR (Fig. 3, top).

The posterior distributions of the parameters from Model 3 are shown in Fig. 3 (bottom left). The median of the posterior distributions was taken as a numerical estimate of the model parameters. The overall intercept was 0.048 with RT-ddPCR and 0.33 with RT-qPCR. A value of zero means that the average measured concentration is one copy (zero  $\log_2$  copies) when the anticipated concentration is one copy. The overall slope was 0.99 with RT-ddPCR and 0.96 with RT-qPCR. A value of 1.0 means that the measured concentration, on average, increases with one  $\log_2$  for every unit increase in  $\log_2$  anticipated concentration.

Between-run variability was assessed by estimating how much 1) the intercept and 2) the slope varied between different runs. The SD of the intercept shifts was 0.018 with RT-ddPCR and 0.49 with RT-qPCR. The SD of the slope shifts was 0.0040 with RT-ddPCR and 0.073 with RT-qPCR. A value of zero would indicate that there is no variation at all between runs. The within-run variability is shown in Fig. 3 (bottom right). At the most concentrated dilution level, the within-run SD was 0.21 with RT-ddPCR and 0.26 with RT-qPCR.

### 3.7. Matrix effects

Matrix effects were assessed in oyster, raspberry, blueberry and leafy-green vegetable extracts spiked with viral RNA from HAV. All samples met the acceptance criterion of less than 75 % inhibition, and none of the matrices caused any major reduction in quantification (Fig. 4). Overall, the average inhibitory effect was 8.1 % for RT-ddPCR, 20 % for RT-qPCR and 5.9 % for RT-qPCR, dd-kit. None of the matrices reduced PCR performance in terms of e.g. decreased separation between the positive and negative droplet populations (for RT-ddPCR) or abnormal amplification curves (for RT-qPCR). No positive signals were detected in the un-spiked matrices.

### 3.8. Sensitivity and quantitative agreement

In total, 51 serum or plasma specimens from naturally infected persons and one naturally contaminated strawberry sample were tested. Among these samples, the overall sensitivity was 90 % (47/52) (95 % CI 78–96) when using RT-ddPCR and 88 % (46/52) (95 % CI 76–95) when

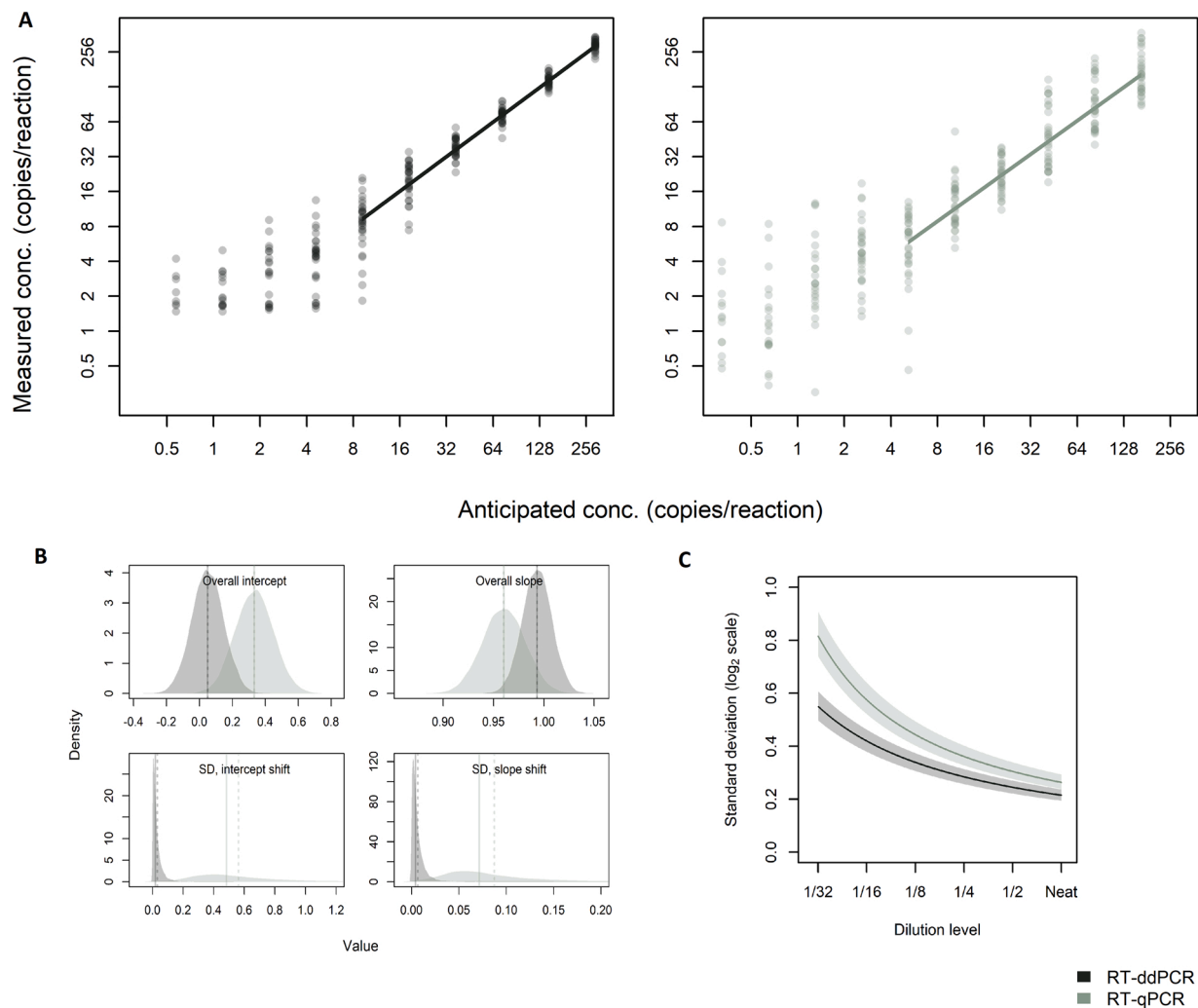


**Fig. 3.** Quantitative detection. **A:** Measured concentration versus dilution level. Dots represent observed values; eight samples were included for each method, dilution level and run, and four runs were performed in total. The solid lines represent the linear predictors as estimated by posterior mean parameter values from Model 3. **B:** Posterior distributions from Model 3. The solid lines indicate means and the dotted lines indicate medians. **C:** Precision within runs, as predicted by Model 3. To enable direct comparison of the two methods, the within-run SD is plotted against dilution level, instead of anticipated concentration. The solid lines are the median of the posterior distribution of the within-run SD, and the shaded area holds the true value of the within-run SD with 95 % probability. Translated to anticipated concentration, the range on the x-axis corresponds to 9.2–293 copies/reaction in RT-ddPCR and 5.2–166 copies/reaction in RT-qPCR. Black: RT-ddPCR, green: RT-qPCR.

using RT-qPCR. The strawberry sample tested positive with both methods. All samples that tested negative with RT-ddPCR also tested negative with RT-qPCR, and all negative samples belonged to genotype IB (the most common genotype in the sample set). Hence, for genotype IB specifically, the sensitivities were 81 % (21/26) (95 % CI: 60–92) when using RT-ddPCR and 77 % (20/26) (95 % CI: 56–90) when using RT-qPCR. For the samples that tested positive with both methods, the concentrations obtained by RT-ddPCR were on average 72 % of those obtained by RT-qPCR (Fig. 5). The inhibitory effect of each sample was monitored through target-specific EC RNA. The mean inhibitory effect was 5.1 % (95 % CI: 0.85–9.12) for RT-ddPCR and -13 % (95 % CI: -19.57 to -9.48) for RT-qPCR. A negative value means that the EC RNA in the sample well showed a higher concentration than the EC RNA in the control well.

### 3.9. Comparison with a standard method

The assay developed in this study was compared with the assay recommended in the ISO method (ISO, 2017) by analysing an *in vitro*-transcribed RNA template containing the target sequence for both

assays. The new assay displayed improved RT-qPCR performance in terms of lower C<sub>q</sub> values, increased end-point fluorescence levels and steeper slopes at the exponential phase of the amplification curves (Fig. 6). A (rough) comparison of LOD revealed that the assay developed in this study appeared to perform at least equally well to the ISO assay (Table 3).

## 4. Discussion

Several recent multi-country outbreaks have highlighted the significance of foodborne transmission of HAV (Enkirch et al., 2018; Nordic, 2013; Rajiuddin et al., 2018). Molecular methods that provide sensitive detection and precise enumeration of foodborne viruses are important for epidemiological tracing in outbreak investigations and for food safety control. Unfortunately, outbreak investigations are often challenging, the presence of HAV is seldom confirmed in food due to difficulties of trace-back and methodological limitations, the incubation period of hepatitis A is long (15–50 days) and identification of a single source or food producer can be difficult due to complex supply chains (Enkirch et al., 2018). In addition, food samples often contain inhibitory

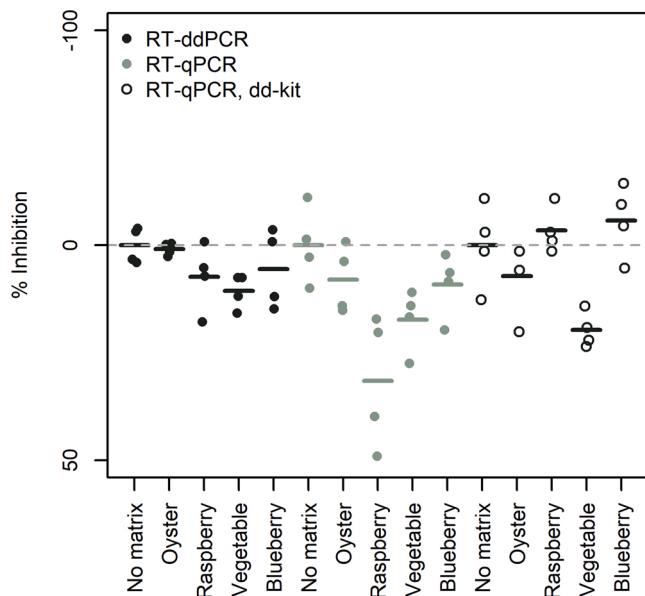


**Fig. 4.** Matrix effects from food sample extracts. A value of 0 indicates no matrix effect and a positive value indicates that the food sample extract caused a reduction in quantification compared with the control without food sample extract. Dots represent observed values ( $n = 4$  per method and food type) and solid lines represent mean values.

substances for RT and/or PCR, which can cause false negative results.

We found that the 5' UTR was the most conserved genomic region (Fig. 1), as reported in a previous study (Costafreda et al., 2006). Hence, several RT-qPCR assays have been developed to target the 5' UTR of HAV, e.g. (Costa-Mattioli et al., 2002; Costafreda et al., 2006; El Galil et al., 2005; Jothikumar et al., 2005; Villar et al., 2006), including the assay recommended in the ISO method. The *in silico* inclusivity analysis revealed that our assay matched perfectly with 76 % (370/487) of the sequences of interest. This is considerably better than the assay recommended in the ISO method (ISO, 2017), which matched perfectly with 59/119 (50 %) of the sequences of interest (Persson et al., 2019). The

assay recommended by the ISO method has previously been found to mismatch to all genotype III strains found in GenBank, causing underestimation of the target concentration and impaired LOD95 % (Persson et al., 2019). The global emergence of genotype III strains (Bosch et al., 2016; Miyamura et al., 2012; Mukomolov et al., 2012) justifies updating of the detection method, especially as the virus concentration in contaminated foods often appears to be below LOD95 %. With the new assay developed in this study, the most common mismatch was a single C (primer) to A (template) mismatch located near the 5' end of the forward primer region. Due to its location near the 5' end, we consider it unlikely that it will affect detection and quantification to any major extent. Furthermore, the mismatch identified is a pyrimidine to purine combination, which is known to have less influence on PCR quantification than pyrimidine to pyrimidine and purine to purine mismatches

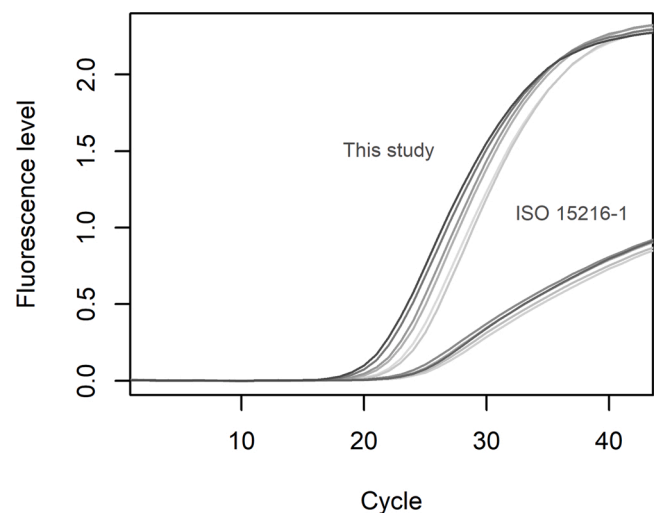


**Fig. 6.** RT-qPCR performance of the assay developed in this study and the assay recommended in the ISO method. RT-qPCR was performed with a gradually increased volume of raspberry matrix, ranging from 0  $\mu$ L (darkest colour) to 5.0  $\mu$ L (lightest colour), in each well.

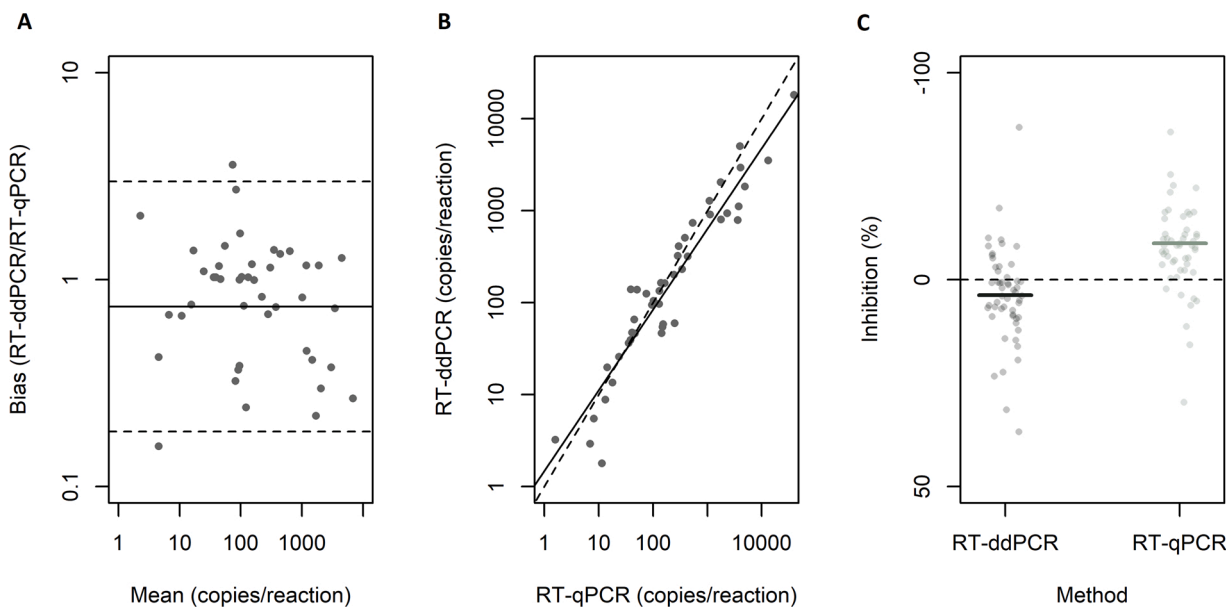


**Fig. 5.** Analysis of hepatitis A virus (HAV)-positive samples. **A:** quantitative agreement between RT-ddPCR and RT-qPCR. The solid line represents the mean value and the dotted lines represent mean  $\pm$  1.96 SD. **B:** Concentration in RT-ddPCR versus concentration in RT-qPCR. The solid line represents the observed relationship and the dotted line represents the line of equality. **C:** Inhibition. A value of 0 indicates no inhibition and a positive value indicates an inhibitory effect. The dots represent observed values and the horizontal lines represent mean values.

**Table 3**

RT-qPCR detection of a dilution series of *in vitro*-transcribed RNA using the assay developed in this study and the assay recommended in the ISO method. Four replicate wells of each concentration were analysed with each assay.

Dilution level	This study			ISO 15216–1		
	Cq mean	Cq SD	Positive/total	Cq mean	Cq SD	Positive/total
Neat	21.9	0.08	4/4	24.8	0.16	4/4
1/10	25.1	0.30	4/4	28.1	0.25	4/4
1/100	28.7	0.28	4/4	31.8	0.43	4/4
1/1000	32.1	0.40	4/4	35.5	1.08	4/4
1/10 000	34.8	0.64	4/4	39.4	–	1/4
1/100 000	–	–	0/4	39.3	–	1/4

(Christopherson et al., 1997). All other mismatches that are not explicitly mentioned in this paper were not frequently occurring (i.e. present in only one or a few sequences) and were considered less severe. The sensitivity test did not indicate any difficulties of detecting genotype III (13/13 samples were positive, see Sections 2.12.2 and 3.8).

As most food samples contain low concentrations of viral RNA, it is desirable to use an assay that can detect as low target levels as possible. We found that RT-qPCR performed somewhat better than RT-ddPCR in terms of probability of detection, but the difference was small; LOD95 % was only 1.1 times higher with RT-ddPCR. It is important to note that different kits and cycling conditions were used for RT-ddPCR and RT-qPCR, as there was only one one-step RT-PCR kit available for our RT-ddPCR instrument at the time of this study. The choice of RT-PCR chemistry can have major impacts on the probability of detection. Therefore, these results should not be taken as a direct comparison between RT-ddPCR and RT-qPCR. Rather, it can be concluded that the RT-qPCR protocol for this assay is preferable to the corresponding RT-ddPCR protocol if qualitative detection of low levels of HAV is the main interest. Whether or not this depends on the choice of instrument, RT-PCR chemistry or other factors was not studied here. The RT-qPCR kit used in this study is used by the majority of national reference laboratories for foodborne viruses within the EU (Ramia Molin, European Union Reference Laboratory for Foodborne Viruses, personal communication 2019) and is recommended in the ISO method (ISO, 2017).

The quantification approaches of RT-ddPCR and RT-qPCR [with DNA quantification standards, as recommended in the ISO method (ISO, 2017)], does not take RT efficiency into account (Sanders et al., 2013). Hence, the concentrations reported in this study and the estimated LOD95 % values reflect the number of amplifiable cDNA copies in the sample. The concentration of target nucleic acid in the original sample may be several orders of magnitude higher than the measured concentration, due to viral loss in the sample processing steps before RT-PCR. In addition, the efficiency of RT may vary between e.g. different assays, priming strategies, enzyme kits and sample types (Bustin et al., 2009; Sanders et al., 2013; Schwaber et al., 2019; Stahlberg et al., 2004).

One of our main objectives was to compare the precision of RT-ddPCR and RT-qPCR. From Model 3, which allowed us to study and compare precision over a range of target concentrations, we found that the precision was greater for RT-ddPCR, both within and especially between runs (see Fig. 3 and Fig. S3 in Supplementary Material). In fact, RT-ddPCR showed barely any variation at all between runs, with the intercept and the slope of the linear predictor showing almost no change between runs (SD of the intercept shift and the slope shift was close to zero) (Fig. 3, bottom left). To minimise variability in RT-qPCR, it is often recommended to analyse all samples that have to be compared within the same run (referred to as the “sample maximisation method”) (Hellemans et al., 2007; Ruijter et al., 2015). Our results suggest that this strategy does not need to be considered in RT-ddPCR analysis. Moreover, the overall improved precision of RT-ddPCR will result in lower measurement uncertainty of the results. This allows for detection of e.g. smaller changes in viral concentrations over time, which has direct implications for both food safety and control as well as for clinical

studies, to e.g. better understand the course of infection and the effect of antiviral drugs.

The advantage with our model (Model 3), as opposed to a conventional linear mixed effects model, is that it takes the heteroscedastic nature of PCR data into account. We selected a simple equation to describe the inverse proportional relationship between template concentration and SD, and it fitted well within the concentration span we investigated. One could have fitted some kind of Poisson-based model, to more accurately represent the underlying error structure. However, we opted for the canonical way of modelling data like this, i.e. using a log-normal model, and leave a thorough investigation of a Poisson-based model as a topic of future research.

The higher precision of RT-ddPCR could be attributable to the digital end-point detection technique. Random differences in PCR efficiency between wells will affect when (at which cycle) detectable fluorescent signals are emitted. In RT-qPCR, such differences will influence the Cq value and hence affect the quantification of the template. However, in RT-ddPCR, quantification will not be affected as long as the fluorescence level of the positive droplets remains above the threshold for a positive droplet when the reaction is completed.

Between-run variation can arise from random differences in e.g. primer and reagent concentrations, cDNA yield from the RT step, and temperature and timing of the different PCR steps (Ruijter et al., 2015). The greater between-run precision of RT-ddPCR may be explained by the digital end-point detection technique mentioned above. However, the difference may be explained to some extent by how calibration curves were used in RT-qPCR. Each run was performed with a DNA standard in duplicate wells at each concentration. Small random differences in Cq values in the standard wells can affect the slope and the intercept of the calibration curve, especially if few replicates are used at each concentration and if the standard contains only a few concentrations. Small changes in the slope of the calibration curve will have a negligible effect on the concentration of samples with Cq values in the middle of the calibration curve, but a greater effect on the concentration of samples with Cq values at the extreme ends of, and outside, the calibration curve. Many of the samples in the evaluation study were at the lower extreme or outside the calibration curve. Again, different kits, instruments and cycling conditions were used for RT-ddPCR and RT-qPCR. Therefore, the possibility that the differences were due to reaction conditions and kit, rather than detection technique, cannot be ruled out. However, it can be concluded that the RT-ddPCR protocol for this assay is strongly preferable if precise quantification is of primary interest.

Four representative food types were selected for investigation of matrix effects. No major matrix effect was detected, in either RT-ddPCR or RT-qPCR. It has previously been reported that RT-ddPCR withstands inhibition better than RT-qPCR, due to the digital end-point detection technique (Racki et al., 2014). Here, we found that the performance of RT-ddPCR and RTqPCR, dd-kit appeared similar (Fig. 4), indicating that the method of detection (i.e. end-point versus real-time) did not matter in this case. In this case, it seems as the tolerance to inhibitors was mostly dependent on detection kit and reaction conditions, in favour of the RT-ddPCR kit. However, this conclusion is based on limited results, as only one sample of each food type was included, and none of them caused any major inhibition. The digital end-point detection technique could perhaps be more advantageous in more severely inhibited samples. This warrants for further investigation, as an increased tolerance to inhibitors also improves sensitivity.

Not all HAV-positive patient samples were detected in the sensitivity analysis. All the negative samples belonged to subtype IB, but this was also the most prevalent subtype in the test panel (26/52 samples). False negative results could potentially be due to mismatches, but the *in silico* inclusivity analysis did not indicate any severe mismatches towards genotype IB. There were no quantitative data available for the test panel, so the viral RNA concentration in these samples was not known, and the samples had been subjected to repeated cycles of freeze thawing, which

may have caused degradation of viral RNA. The sensitivity can be improved by increasing the volume used for nucleic acid extraction and RT-PCR and increasing the number of replicate RT-PCR wells, but this was unfortunately not possible due to limited sample volumes. A limitation of this experiment was that not all human sub-genotypes were represented in the panel (IIB and IIIB were missing, and there were only four samples of subgenotype IIA). The inclusion of more samples would have permitted a more robust sensitivity estimate, but the availability of HAV positive samples was limited, and genotype II is rare. In the *in silico* inclusivity analysis, there were only 4/487 sequences that were assigned to genotype II (Table 2). The assay matched perfectly with all four.

In the plasma and serum samples, there was no inhibitory effect in either RT-ddPCR (5 %) or RT-qPCR (-13 %). A possible explanation for the negative inhibitory effect found in RT-qPCR is that the EC RNA in the control well with nuclease-free water may have been sub-optimally reverse-transcribed or amplified. We speculate that this may be due to absence of background RNA in the control wells. The presence of nonhomologous RNA may increase the efficiency of RT, potentially by reducing adsorption of the target molecule to e.g. the pipette tip or the sample well wall (Stahlberg et al., 2004). The negative inhibitory effect has been observed previously for other assays analysed using the same kit and plastic consumables (data not shown). It could also explain why the measured concentrations in RT-ddPCR were higher than in RT-qPCR in the evaluation study (Fig. 3), where highly diluted viral RNA from cell-culture supernatant was used, but not in verification using naturally contaminated samples (Fig. 6).

The assay developed in this study is targeted to a part of the internal ribosomal entry site (IRES) within the 5' UTR (IRES enables cap-independent translation to synthesise viral proteins; the location of IRES in different HAV genomes can be found at: <http://rfam.xfam.org/family/RF00228#tabview=tab1>, accessed on April 25, 2019). IRES forms a strong secondary structure at 37 °C (Brown et al., 1994) and potentially also at 50 and 55 °C, which were the temperatures used during reverse transcription in this study. Secondary structures are important to consider during RT-PCR assay design, as they may decrease the efficiency of reverse transcription by e.g. sterically hindering the reverse primer to bind or causing the reverse transcriptase to stall (Bustin, 2002; Bustin et al., 2009). Here, reverse transcription efficiency was evaluated by analysing a known concentration of *in vitro*-transcribed RNA and linearised plasmid DNA using RT-ddPCR, and comparing the measured concentration with the nominal concentration for both DNA and RNA. In this sense, the assay used in this study did not display impaired performance in comparison with the assay recommended in the ISO method (ISO, 2017), which is also located within the 5' UTR (results are shown in Table S3 in Supplementary Material).

In summary, we developed and evaluated a new method for nucleic acid-based detection of HAV in food samples. By verification against the assay recommended in the ISO method (ISO, 2017), we concluded, based on the test with RNA from an HAV sequence (which matched perfectly with both assays), and a food sample, that the new assay displays considerably better RT-qPCR performance and at least as good LOD as the ISO assay. The assay developed in this study amplifies a product of 91 base pairs, whereas the ISO assay amplifies a product of 157–188 base pairs, depending on the HAV strain. In the evaluation report of the ISO method (Lowther et al., 2017), the long amplicon length has been pointed out as a probable cause of sub-optimal performance, as it became evident that HAV had higher LOD than norovirus. This, in combination with the improved inclusivity discussed earlier, suggests that our assay can be considered a suitable alternative to the assay recommended by the ISO method. The new assay is adapted for both RT-ddPCR and RT-qPCR, but RT-qPCR is generally less expensive and time-consuming than RT-ddPCR, e.g. it requires fewer pipetting steps and less hands-on time by the operator than RT-ddPCR. Therefore, our results suggest that RT-qPCR is preferable for use in the assay if rapid, qualitative detection at low target concentrations is the main interest and that RT-ddPCR is preferable if precise quantification is the

main interest. Although a serological assay directed towards anti-HAV IgM in serum is the standard approach for clinical diagnosis of hepatitis A, RT-ddPCR or RT-qPCR can be used for monitoring viraemia and faecal shedding, to better understand the course of infection or as a screening method in outbreak settings for early diagnosis and to identify asymptomatic carriers (Bower et al., 2000; Nainan et al., 2006; Pintó et al., 2012). Here, we demonstrated that our method is suitable for detection of HAV in human serum samples.

## Funding

The work was funded by the Swedish Civil Contingencies Agency (dnr. 2014–1957). The funding source was not involved in any aspect of study design, data collection, analysis, interpretation of data or manuscript.

## CRedit authorship contribution statement

**Sofia Persson:** Conceptualization, Formal analysis, Investigation, Visualization, Writing - original draft. **Erik Alm:** Conceptualization, Software, Methodology, Writing - review & editing. **Måns Karlsson:** Methodology, Formal analysis, Writing - original draft. **Theresa Enkirch:** Investigation, Resources, Writing - review & editing. **Heléne Norder:** Investigation, Resources, Writing - review & editing. **Ronnie Eriksson:** Investigation, Project administration, Writing - review & editing. **Magnus Simonsson:** Conceptualization, Supervision, Writing - review & editing, Funding acquisition. **Patrik Ellström:** Conceptualization, Supervision, Writing - review & editing.

## Declaration of Competing Interest

The authors reported no declarations of interest.

## Acknowledgements

We are grateful to Felix Wahl at the Department of Mathematics at Stockholm University for insightful comments on the Bayesian modelling approach.

## Appendix A. Supplementary data

Supplementary material related to this article can be found, in the online version, at doi:<https://doi.org/10.1016/j.jviromet.2020.114010>.

## References

- Bland, J.M., Altman, D.G., 1986. Statistical methods for assessing agreement between two methods of clinical measurement. *Lancet* 1, 307–310.
- Bosch, A., Pintó, R.M., Guix, S., 2016. Foodborne viruses. *Curr. Opin. Food Sci.* 8, 110–119.
- Bower, W.A., Nainan, O.V., Han, X., Margolis, H.S., 2000. Duration of viremia in hepatitis A virus infection. *J. Infect. Dis.* 182, 12–17.
- Brown, E.A., Zajac, A.J., Lemon, S.M., 1994. In vitro characterization of an internal ribosomal entry site (IRES) present within the 5' nontranslated region of hepatitis A virus RNA: comparison with the IRES of encephalomyocarditis virus. *J. Virol.* 68, 1066–1074.
- Bustin, S., 2002. Quantification of mRNA using real-time reverse transcription PCR (RT-PCR): trends and problems. *J. Mol. Endocrinol.* 29, 23–39.
- Bustin, S.A., Benes, V., Garson, J.A., Hellemans, J., Huggett, J., Kubista, M., Mueller, R., Nolan, T., Pfaffl, M.W., Shipley, G.L., Vandesompele, J., Wittwer, C.T., 2009. The MIQE guidelines: minimum information for publication of quantitative real-time PCR experiments. *Clin. Chem.* 55, 611–622.
- Calder, L., Simmons, G., Thornley, C., Taylor, P., Pritchard, K., Greening, G., Bishop, J., 2003. An outbreak of hepatitis A associated with consumption of raw blueberries. *Epidemiol. Infect.* 131, 745–751.
- Callejón, R.M., Rodríguez-Naranjo, M.I., Ubeda, C., Hornedo-Ortega, R., García-Parrilla, M.C., Troncoso, A.M., 2015. Reported foodborne outbreaks due to fresh produce in the United States and European Union: trends and causes. *Foodborne Pathog. Dis.* 12, 32–38.
- Carpenter, B., Gelman, A., Hoffman, M.D., Lee, D., Goodrich, B., Betancourt, M., Brubaker, M., Guo, J., Li, P., Riddell, A., 2017. Stan: a probabilistic programming language. *J. Stat. Softw.* 76.

- Carvalho, C., Thomas, H., Balogun, K., Tedder, R., Pebody, R., Ramsay, M., Ngui, S., 2012. A possible outbreak of hepatitis A associated with semi-dried tomatoes, England, July–November 2011. *Eurosurveillance* 17, 20083.
- Charif, D., Lobry, J.R., 2007. SeqinR 1.0-2: A Contributed Package to the R Project for Statistical Computing Devoted to Biological Sequences Retrieval and Analysis, Structural Approaches to Sequence Evolution. Springer, pp. 207–232.
- Christopherson, C., Sninsky, J., Kwok, S., 1997. The effects of internal primer-template mismatches on RT-PCR: HIV-1 model studies. *Nucleic Acids Res.* 25, 654–658.
- Costafreda, M.I., Bosch, A., Pinto, R.M., 2006. Development, evaluation, and standardization of a real-time TaqMan reverse transcription-PCR assay for quantification of hepatitis A virus in clinical and shellfish samples. *Appl. Environ. Microbiol.* 72, 3846–3855.
- Costa-Mattioli, M., Monpoeho, S., Nicand, E., Aleman, M.H., Billaudel, S., Ferre, V., 2002. Quantification and duration of viraemia during hepatitis A infection as determined by real-time RT-PCR. *J. Viral Hepat.* 9, 101–106.
- Coudray-Meunier, C., Fraisse, A., Martin-Latit, S., Guillier, L., Delannoy, S., Fach, P., Perelle, S., 2015. A comparative study of digital RT-PCR and RT-qPCR for quantification of Hepatitis A virus and Norovirus in lettuce and water samples. *Int. J. Food Microbiol.* 201, 17–26.
- D'Andrea, L., Pérez-Rodríguez, F., de Castellarnau, M., Manzanares, S., Lite, J., Guix, S., Bosch, A., Pintó, R., 2015. Hepatitis A virus genotype distribution during a decade of universal vaccination of preadolescents. *Int. J. Mol. Sci.* 16, 6842–6854.
- Edgar, R.C., 2004. MUSCLE: multiple sequence alignment with high accuracy and high throughput. *Nucleic Acids Res.* 32, 1792–1797.
- El Galil, K.H.A., El Sokkary, M., Kheira, S., Salazar, A.M., Yates, M.V., Chen, W., Mulchandani, A., 2005. Real-time nucleic acid sequence-based amplification assay for detection of hepatitis A virus. *Appl. Environ. Microbiol.* 71, 7113–7116.
- Enkirsch, T., Eriksson, R., Persson, S., Schmid, D., Aberle, S.W., Löf, E., Wittesjö, B., Holmgren, B., Johnzon, C., Gustafsson, E.X., 2018. Hepatitis A outbreak linked to imported frozen strawberries by sequencing, Sweden and Austria, June to September 2018. *Eurosurveillance* 23, 1800528.
- Forootan, A., Sjöback, R., Bjorkman, J., Sjögreen, B., Linz, L., Kubista, M., 2017. Methods to determine limit of detection and limit of quantification in quantitative real-time PCR (qPCR). *Biomol. Detect. Quantif.* 12, 1–6.
- HAVNet, 2018. Protocol Molecular Detection and Typing of VP1 Region of Hepatitis A Virus (HAV).
- Hayden, R.T., Gu, Z., Ingersoll, J., Abdul-Ali, D., Shi, L., Pounds, S., Caliendo, A.M., 2013. Comparison of droplet digital PCR to real-time PCR for quantitative detection of cytomegalovirus. *J. Clin. Microbiol.* 51, 540–546.
- Hedman, J., Lavander, M., Salomonsson, E.N., Jinnerot, T., Boiso, L., Magnusson, B., Rådström, P., 2018. Validation guidelines for PCR workflows in bioterrorism preparedness, food safety and forensics. *Accredit. Qual. Assur.* 1–12.
- Hellemans, J., Mortier, G., De Paep, A., Speleman, F., Vandesompele, J., 2007. qBase relative quantification framework and software for management and automated analysis of real-time quantitative PCR data. *Genome Biol.* 8, R19.
- Herman, K., Hall, A., Gould, L., 2015. Outbreaks attributed to fresh leafy vegetables, United States, 1973–2012. *Epidemiol. Infect.* 143, 3011–3021.
- Hindson, C.M., Chevillet, J.R., Briggs, H.A., Gallicchio, E.N., Ruf, I.K., Hindson, B.J., Vessella, R.L., Tewari, M., 2013. Absolute quantification by droplet digital PCR versus analog real-time PCR. *Nat. Methods* 10, 1003–1005.
- Huggett, J.F., Foy, C.A., Benes, V., Emslie, K., Garson, J.A., Haynes, R., Hellemans, J., Kubista, M., Mueller, R.D., Nolan, T., Pfaffl, M.W., Shipley, G.L., Vandesompele, J., Wittwer, C.T., Bustin, S.A., 2013. The digital MIQE guidelines: minimum information for publication of quantitative digital PCR experiments. *Clin. Chem.* 59, 892–902.
- Hutin, Y.J., Pool, V., Cramer, E.H., Nainan, O.V., Weth, J., Williams, I.T., Goldstein, S.T., Gensheimer, K.F., Bell, B.P., Shapiro, C.N., 1999. A multistate, foodborne outbreak of hepatitis A. *New England J. Med.* 340, 595–602.
- ISO, 1994. In: ISO (Ed.), ISO 5725-2 Accuracy (Trueness and Precision) of Measurement Methods and Results – Part 2: Basic Method for the Determination of Repeatability and Reproducibility of a Standard Measurement Method.
- ISO, 2017. In: ISO (Ed.), ISO 15216-1 Microbiology of the Food Chain - Horizontal Method for Determination of Hepatitis A Virus and Norovirus Using Real-Time PCR, Part 1: Method for Quantification. Switzerland.
- Jiang, X., Kanda, T., Wu, S., Nakamoto, S., Saito, K., Shirasawa, H., Kiyohara, T., Ishii, K., Wakita, T., Okamoto, H., 2014. Suppression of La antigen exerts potential antiviral effects against hepatitis A virus. *PLoS One* 9, e101993.
- Jothikumar, N., Cromeans, T., Sobsey, M., Robertson, B., 2005. Development and evaluation of a broadly reactive TaqMan assay for rapid detection of hepatitis A virus. *Appl. Environ. Microbiol.* 71, 3359–3363.
- Lemon, S.M., Jansen, R.W., Brown, E.A., 1992. Genetic, antigenic and biological differences between strains of hepatitis A virus. *Vaccine* 10, S40–S44.
- Lowther, J.A., Bosch, A., Butot, S., Ollivier, J., Made, D., Rutjes, S.A., Hardouin, G., Lombard, B., In't Veld, P., Leclercq, A., 2017. Validation of ISO method 15216 part 1 - quantification of hepatitis A virus and norovirus in food matrices. *Int. J. Food Microbiol.*
- Martin, A., Lemon, S.M., 2006. Hepatitis A virus: from discovery to vaccines. *Hepatology* 43.
- Mast, E.E., Alter, M.J., 1993. Epidemiology of viral hepatitis: an overview. *Semin. Virol.* 4, 273–283.
- Matz, M.V., Wright, R.M., Scott, J.G., 2013. No control genes required: Bayesian analysis of qRT-PCR data. *PLoS One* 8.
- Miyamura, T., Ishii, K., Kanda, T., Tawada, A., Sekimoto, T., Wu, S., Nakamoto, S., Arai, M., Fujiwara, K., Imazeki, F., 2012. Possible widespread presence of hepatitis A virus subgenotype IIIA in Japan: recent trend of hepatitis A causing acute liver failure. *Hepatol. Res.* 42, 248–253.
- Mukomolov, S., Kontio, M., Zheleznova, N., Jokinen, S., Sinayskaya, E., Stalevskaya, A., Davidkin, I., 2012. Increased circulation of hepatitis A virus genotype IIIA over the last decade in St Petersburg, Russia. *Journal of medical virology* 84, 1528–1534.
- Murray, P.R., Rosenthal, K.S., Pfaller, M.A., 2015. *Medical Microbiology*. Elsevier Health Sciences.
- Nainan, O.V., Xia, G., Vaughan, G., Margolis, H.S., 2006. Diagnosis of hepatitis A virus infection: a molecular approach. *Clin. Microbiol. Rev.* 19, 63–79.
- Nordic, C.O.I.T., 2013. Joint analysis by the Nordic countries of a hepatitis A outbreak, October 2012 to June 2013: frozen strawberries suspected. *Euro surveillance: bulletin European sur les maladies transmissibles= European Communicable Disease Bulletin* 18.
- Pérez-Sautu, U., Costafreda, M.I., Lite, J., Sala, R., Barrabeig, I., Bosch, A., Pintó, R.M., 2011. Molecular epidemiology of hepatitis A virus infections in Catalonia, Spain, 2005–2009: circulation of newly emerging strains. *J. Clin. Virol.* 52, 98–102.
- Persson, S., Eriksson, R., Lowther, J., Ellstrom, P., Simonsson, M., 2018. Comparison between RT droplet digital PCR and RT real-time PCR for quantification of noroviruses in oysters. *Int. J. Food Microbiol.* 284, 73–83.
- Persson, S., Karlsson, M., Borsch-Remiers, H., Ellström, P., Eriksson, R., Simonsson, M., 2019. Missing the match might not cost you the game: primer-template mismatches studied in different hepatitis A virus variants. *Food Environ. Virol.* 1–12.
- Petrignani, M., Harms, M., Verhoef, L., Van Hunen, R., Swaan, C., Van Steenberghe, J., Boxman, I., Sala, R.P., Ober, H., Vennema, H., 2010. Update: a food-borne outbreak of hepatitis A in the Netherlands related to semi-dried tomatoes in oil, January–February 2010. *Eurosurveillance* 15, 19572.
- Pintó, R.M., D'Andrea, L., Pérez-Rodríguez, F.J., Costafreda, M.I., Ribes, E., Guix, S., Bosch, A., 2012. Hepatitis A virus evolution and the potential emergence of new variants escaping the presently available vaccines. *Future Microbiol.* 7, 331–346.
- R, C.T., 2020. R: A Language and Environment for Statistical Computing. A.R.F.F.S.C, Vienna.
- Racki, N., Dreo, T., Gutierrez-Aguirre, I., Blejec, A., Ravnkar, M., 2014. Reverse transcriptase droplet digital PCR shows high resilience to PCR inhibitors from plant, soil and water samples. *Plant Methods* 10, 42.
- Rajjuddin, S.M., Midgley, S.E., Jensen, T., Müller, L., Schultz, A.C., 2018. Detection of hepatitis A virus by direct extraction of viral RNA from dates implicated in a disease outbreak in Denmark. *Danish Microbiol. Soc. Annual Congress 2018*, 49–49.
- Reid, T., Robinson, H., 1987. Frozen Raspberries and Hepatitis A. *Epidemiology & Infection*, 98, pp. 109–112.
- Rosenblum, L.S., Mirkin, I.R., Allen, D.T., Safford, S., Hadler, S.C., 1990. A multifocal outbreak of hepatitis A traced to commercially distributed lettuce. *Am. J. Public Health* 80, 1075–1079.
- Ruijter, J.M., Villaiba, A.R., Hellemans, J., Untergasser, A., van den Hoff, M.J., 2015. Removal of between-run variation in a multi-plate qPCR experiment. *Biomol. Detect. Quantif.* 5, 10–14.
- Sánchez, G., Pintó, R.M., Vanaclocha, H., Bosch, A., 2002. Molecular characterization of hepatitis A virus isolates from a transcontinental shellfish-borne outbreak. *J. Clin. Microbiol.* 40, 4148–4155.
- Sanders, R., Mason, D.J., Foy, C.A., Huggett, J.F., 2013. Evaluation of digital PCR for absolute RNA quantification. *PLoS One* 8, e75296.
- Scavia, G., Alfonsi, V., Taffon, S., Escher, M., Bruni, R., De Medici, D., Di Pasquale, S., Guizzardi, S., Cappelletti, B., Iannazzo, S., 2017. A large prolonged outbreak of hepatitis A associated with consumption of frozen berries, Italy, 2013–14. *J. Med. Microbiol.* 66, 342–349.
- Schrader, C., Schielke, A., Ellerbroek, L., Johne, R., 2012. PCR inhibitors—occurrence, properties and removal. *J. Appl. Microbiol.* 113, 1014–1026.
- Schwaber, J., Andersen, S., Nielsen, L., 2019. Shedding light: the importance of reverse transcription efficiency standards in data interpretation. *Biomol. Detect. Quantif.* 17, 100077.
- Sedlak, R.H., Nguyen, T., Palileo, I., Jerome, K.R., Kuypers, J., 2017. Superiority of digital reverse Transcription-PCR (RT-PCR) over real-time RT-PCR for quantitation of highly divergent human rhinoviruses. *J. Clin. Microbiol.* 55, 442–449.
- Shannon, C.E., 1951. Prediction and entropy of printed English. *Bell Syst. Tech. J.* 30, 50–64.
- Stahlberg, A., Hakansson, J., Xian, X., Semb, H., Kubista, M., 2004. Properties of the reverse transcription reaction in mRNA quantification. *Clin. Chem.* 50, 509–515.
- Stan, D.T., 2020. RStan: The R Interface to Stan.
- Strain, M.C., Lada, S.M., Luong, T., Rought, S.E., Gianella, S., Terry, V.H., Spina, C.A., Woelk, C.H., Richman, D.D., 2013. Highly precise measurement of HIV DNA by droplet digital PCR. *PLoS One* 8, e55943.
- Villar, L.M., de Paula, V.S., Diniz-Mendes, L., Lampe, E., Gaspar, A.M.C., 2006. Evaluation of methods used to concentrate and detect hepatitis A virus in water samples. *J. Virol. Methods* 137, 169–176.
- Win, N.N., Kanda, T., Ogawa, M., Nakamoto, S., Haga, Y., Sasaki, R., Nakamura, M., Wu, S., Matsumoto, N., Matsuoka, S., 2019. Superinfection of hepatitis A virus in hepatocytes infected with hepatitis B virus. *Int. J. Med. Sci.* 16, 1366.